IOP Publishing Journal of Physics: Condensed Matter
J. Phys.: Condens. Matter **32** (2020) 285803 (6pp) https://doi.org/10.1088/1361-648X/ab7e5a

Magnetic couplings and magnetocaloric effect in the GdTX (T=Sc, Ti, Co, Fe; X=Si, Ge) compounds

Daniel J García[1,2,4], Verónica Vildosola[1,3] and Pablo S Cornaglia[1,2]

[1] Consejo Nacional de Investigaciones Científicas y Técnicas (CONICET), Argentina
[2] Centro Atómico Bariloche and Instituto Balseiro, CNEA, 8400 Bariloche, Argentina
[3] Centro Atómico Constituyentes, CNEA, Buenos Aires, Argentina

E-mail: garciad@cab.cnea.gov.ar

Received 16 December 2019, revised 19 February 2020
Accepted for publication 10 March 2020
Published 15 April 2020

Abstract

We compute the magnetocaloric effect (MCE) in the GdTX (T = Sc, Ti, Co, Fe; X = Si, Ge) compounds as a function of the temperature and the external magnetic field. To this end we use a density functional theory approach to calculate the exchange–coupling interactions between Gd^{3+} ions on each compound. We consider a simplified magnetic Hamiltonian and analyze the dependence of the exchange couplings on the transition metal T, the p-block element X, and the crystal structure (CeFeSi-type or CeScSi-type). The most significant effects are observed for the replacements Ti $\rightarrow$ Sc or Fe $\rightarrow$ Co which have an associated change in the parity of the electron number in the three dimensional level. These replacements lead to an antiferromagnetic contribution to the magnetic couplings that reduces the Curie temperature and can even lead to an antiferromagnetic ground state. We solve the magnetic models through mean field and Monte Carlo calculations and find large variations among compounds in the magnetic transition temperature and in the magnetocaloric effect, in agreement with the available experimental data. The magnetocaloric effect shows a universal behavior as a function of temperature and magnetic field in the ferromagnetic compounds after a scaling of the relevant energy scales by the Curie temperature T_C.

Keywords: magnetocaloric effect, RTX compounds, DFT, Monte Carlo

(Some figures may appear in colour only in the online journal)

1. Introduction

Gadolinium based compounds, in particular those in the GdTX family [1], have been the subject of numerous theoretical [2–5] and experimental [6–11] studies because of their potential use in refrigeration at room temperature using the magnetocaloric effect. The strong magnetocaloric properties of Gd systems are due to the large spins in the 4f Gd^{3+} ions and the exchange couplings between them that lead to magnetic phase transitions. A giant magnetocaloric effect is observed in $Gd_5(Si_2Ge_2)$ at room temperature, associated with the presence of a first order ferromagnetic (I) $\leftrightarrow$ ferromagnetic (II) transition at $T \simeq 276$ K [12]. Pure gadolinium, which is also a strong magnetocaloric material at room temperature, presents a second order Curie transition at $T_C = 294$ K to a ferromagnetic ground state.

The magnetocaloric effect (MCE) is generally quantified by the entropy change $\Delta S_m = S(H) - S(0)$, when an external magnetic field H is applied. To obtain a large MCE a high sensitivity of the material to magnetic field changes is required. This is the case, e.g., for temperatures close to a paramagnetic–ferromagnetic transition temperature where the MCE acquires its maximum values. For magnetic cooling applications it is important to maximize the MCE at the operation temperatures. A route to attain this goal is to control the magnetic transition temperature through the magnetic couplings

[4] Author to whom any correspondence should be addressed

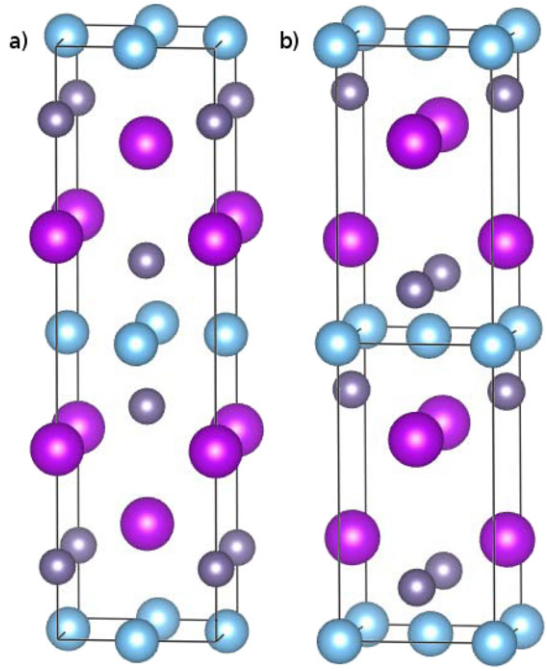

Figure 1. Crystal structures: (a) CeScSi-type (b) CeFeSi-type. The rare earth atoms are represented by the larger spheres, the p-block atoms by the smallest spheres and the transition metal atoms by the middle size spheres.

which are determined by the conduction band structure and its occupancy.

The ternary RTX compounds (where R is a rare earth), T is a transition metal and X is a p-block element such as Si, Ge, Sb) present several examples of large MCE compounds. GdFeSi is a ferromagnet below $T_C = 118\,K$ where the MCE attains its maximum value $\Delta S_M = -22.3\,J\,kg^{-1}\,K = -0.42R$ ($\Delta H = 9$Tesla), GdScSi and GdScGe are also ferromagnets with $T_C = 318$ K and $\Delta S_M = -2.5\,J\,kg^{-1}\,K = -0.047R$ and $T_C = 320\,K$ and $\Delta S_M = -3.3\,J\,kg^{-1}\,K = -0.062R$ for $\Delta H =$ 2Tesla, respectively. GdCoSi is however an antiferromagnet with $T_N = 220$ K and a low MCE [13–16].

Among the variety of RTX crystal structures, we will focus on the tetragonal CeFeSi-type (space group *P4/nmm*) and CeScSi-type (space group *I4/mmm*) R–X–T_2–X–R structures (see figure 1) and analyze the role of T and X in the magnetic properties for the R = Gd case. As we show below, the results of this analysis will prove helpful interpreting the experimental results for other rare earths.

2. Magnetic ground state and coupling constants

We performed density functional theory (DFT) total-energy calculations of the GdTX (T = Sc, Ti, Co, Fe; X = Si, Ge) compounds which indicate a ground state with magnetic moments localized at the Gd^{3+} ions and allowed us to estimate the strength of the Gd–Gd magnetic interactions. We solved the resulting magnetic model to obtain the magnetic contribution to the specific heat, the magnetocaloric effect, and the Néel or Curie transition temperature.

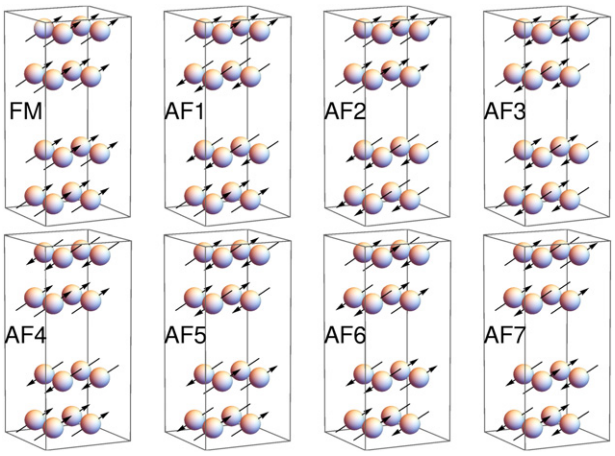

Figure 2. Magnetic configurations proposed for the CeFeSi-type structures to determine the ground state and obtain the exchange coupling parameters. The spheres correspond to Gd ions and the orientation of the Gd^{3+} 4f magnetic moments is indicated by black arrows. An analogous set of magnetic configurations was used for the CeScSi-type structures.

2.1. Technical details of the DFT calculations

The total-energy calculations were performed using the generalized gradient approximation (GGA) of Perdew, Burke and Ernzerhof for the exchange and correlation functional as implemented in the WIEN2k code [17, 18]. A local Coulomb repulsion was included in the Gd 4f shell and treated using GGA + U which is a reasonable approximation for these highly localized states. Due to the localized character of the 4f electrons, the fully localized limit was used for the double counting correction [19]. We described using the DFT + U approximation the local Coulomb and exchange interactions with a single effective local repulsion $U_{eff} = U - J_H = 6$ eV, which has been successfully used in bulk Gd and other Gd compounds [20–25]. The APW + local orbitals method of the WIEN2k code was used for the basis functions [17]. We used 1200 k-points in the Brioullin zone for the full optimization of the crystal structures, and 200 k-points for the $2 \times 2 \times 2$ supercell total-energy calculations of the different magnetic configurations. The magnetic moments are localized on the Gd 4f orbitals and no significant magnetic moment is obtained in the transition metal[5].

2.2. Magnetic structure of the ground state and coupling constants

We explored different static configurations for the magnetic moments which are presented in figure 2 for the CeFeSi-type structures. The magnetic configurations used for the CeScSi-type structures are completely analogous, with the

[5] The spin polarization on the transition metal of each compound was estimated from spin dependent DFT calculations projecting on the transition metal atomic orbitals. We found values between 0 and $0.8\mu_B$ depending on the magnetic configuration of the Gd^{3+} 4f magnetic moments and the transition metal. We expect the magnetocaloric properties of these compounds to be dominated by the much larger local magnetic moment in the Gd^{3+} ions ($\sim 8\mu_B$).

Table 1. Relative energy ΔE (in K) with respect to the ground state for the magnetic configurations of figure 2 for a DFT cell with 16 Gd^{3+} ions. The AF3 configuration is unstable for GdFeSi. The underlined compounds correspond to the CeFeSi-type structure, and the rest to the CeScSi-type structure.

	GdFeSi	GdCoSi	GdTiSi	GdTiGe	GdTiGe	GdScGe	GdScSi
FM	0	198	305	424	0	0	0
AF1	43	891	1608	1459	1967	1551	1537
AF2	220	0	0	0	1013	377	370
AF3	—	711	1339	1442	1941	1220	1217
AF4	466	788	1609	1552	2197	1564	1546
AF5	244	661	1183	1281	2001	1223	1200
AF6	243	660	1183	558	1942	1220	1217
AF7	302	704	1572	1476	2071	1462	1431

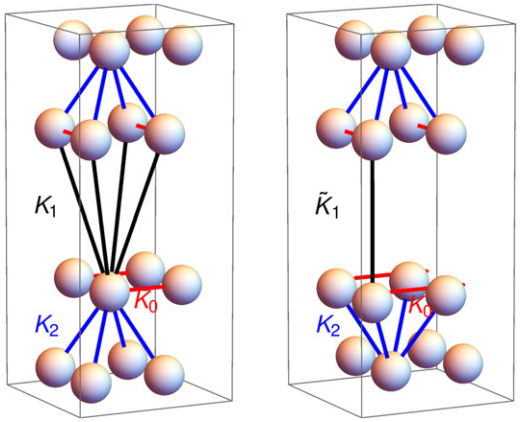

Figure 3. Magnetic couplings considered in the simplified model. The lines connect pairs of Gd atoms that are magnetically coupled (to avoid overloading the plot, not all couplings are drawn, but can be inferred from symmetry considerations) through the exchange coupling parameters K_0, K_1 (only for the CeFeSi-type structure), $\tilde{K}_1$ (only for the CeScSi-type structure), and K_2, as indicated in the figure.

same relative orientation of the magnetic moments inside each Gd layer and between the layers. The lowest energy configuration is identified as the magnetic ground state, which in all the analyzed cases corresponds to the type of order experimentally observed [26–32]: a ferromagnet for GdFeSi, GdTiGe (*I4/mmm*), GdScGe and GdScSi, and an A-type antiferromagnet for GdCoSi, GdTiSi, and GdTiGe (*P4/nmm*) with the magnetic moments of the Gd on each bilayer aligned ferromagnetically, and each bilayer aligned antiferromagnetically with its nearest neighbouring bilayers. The energy differences between a given magnetic moment configuration and the lowest energy one are presented, for each compound, in table 1.

In these metallic compounds, the dominant Gd–Gd magnetic interactions are due to a Ruderman–Kittel–Kasuya–Yosida (RKKY) coupling between the Gd's magnetic moments through exchange interactions with the conduction electrons, which decay in three dimensional (3d) systems as an inverse third power of the inter Gd distance [33–35]. DFT calculations of the RKKY couplings in GdFeSi in reference [4] suggests an even faster decay with increasing inter Gd distance. As it is customary we considered

Table 2. Magnetic energy as a function of the magnetic-exchange couplings for the different magnetic configurations considered in the CeFeSi-type and the CeScSi-type structures. $J = 7/2$ is the angular momentum of the Gd^{3+} ion 4f electrons.

	CeFeSi-type	CeScSi-type
E^{m}_{FM}/J^2	$-4(K_0 + K_1 + K_2)$	$-4K_0 - \tilde{K}_1 - 4K_2$
E^{m}_{AF1}/J^2	$-4(K_0 + K_1 - K_2)$	$-4K_0 - \tilde{K}_1 + 4K_2$
E^{m}_{AF2}/J^2	$-4(K_0 - K_1 + K_2)$	$-4K_0 + \tilde{K}_1 - 4K_2$
E^{m}_{AF3}/J^2	0	$-\tilde{K}_1$
E^{m}_{AF4}/J^2	$-4(K_0 - K_1 - K_2)$	$-4K_0 + \tilde{K}_1 + 4K_2$
E^{m}_{AF5}/J^2	0	$\tilde{K}_1$
E^{m}_{AF6}/J^2	0	$-\tilde{K}_1$
E^{m}_{AF7}/J^2	$4K_0$	$4K_0 + \tilde{K}_1$

Table 3. Calculated exchange couplings (in K) and the calculated Néel temperatures. Boldface indicates interplane couplings. Shaded cells correspond to Curie temperatures. The experimental Néel T_N^{exp} are presented as a reference. The superscripts indicate the references from which the experimental values were extracted: a = [16], b = [29], c = [27], d = [30], e = [31], f = [32].

	GdFeSi	GdCoSi	GdTiSi	GdTiGe	GdTiGe	GdScGe	GdScSi
K_0	1.6	4.4	10.3	8	17.0	10.6	10.4
$\mathbf{K_1}$	**4.5**	**−2.4**	**−3.2**	**−4.1**	—	—	—
$\tilde{\mathbf{K}}_1$	—	—	—	—	**26.5**	**9.2**	**8.4**
K_2	1.7	11.5	21.9	18.7	30.9	23.7	23.5
T_c^{MF}	163	386	745	646	1145	766	756
T_c^{MC}	117.5	284.5	554.5	477	637	404	395
T_c^{QMC}	154	363	710	620	840	555	530
T_c^{exp}	118[a]	175[b]	400[c]	412[d]	376[e]	320[f]	318[f]

a finite set of exchange interactions. The eight magnetic configurations considered allow us to calculate up to seven exchange couplings. We found that an accurate description of the system is obtained using a simplified model for the magnetic interaction between Gd^{3+} magnetic moments, with three coupling constants (see figure 3) [27, 36]: an exchange coupling K_0 between nearest neighbour Gd atoms on each Gd layer (which is a square lattice), a coupling K_2 between nearest neighbours in different layers of the bilayer, and a nearest neighbour coupling between Gd in different bilayers. For the latter coupling there are two possibilities depending on the lattice type: K_1 associated with 4 neighbours in the CeFeSi-type structure, and $\tilde{K}_1$ associated with a single neighbour in the CeScSi-type structure (see figure 3). We found that including up to three additional magnetic couplings in the model only lead to minor quantitative differences in the calculated properties. The magnetic energy per Gd^{3+} ion is presented in table 2 for the magnetic configurations of figure 2.

The energy differences between magnetic configurations calculated from first principles can be combined with table 2 to obtain the coupling parameters through a least squares analysis. The obtained couplings for the different compounds are presented in table 3. For all the studied compounds, the intra-bilayer couplings K_0 and K_2 are positive which indicates that in all cases the Gd magnetic moments in a given bilayer order

ferromagnetically. The interbilayer couplings can be positive as in GdFeSi, GdTiGe (*I4/mmm*), GdScGe, and GdScSi leading to a ferromagnetic ground state or negative as in GdCoSi, GdTiSi, and GdTiGe (*P4/nmm*) which results in an A-type antiferromagnet. The replacement Si $\rightarrow$ Ge does not lead to a significant change in the exchange couplings of GdTiSi and GdScSi which is consistent with the very weak change in the transition temperatures observed in these compounds upon Si $\rightarrow$ Ge replacement. The replacements Fe $\rightarrow$ Co in GdFeSi and Ti $\rightarrow$ Sc in GdTiGe produce, however, a change in the sign of the interbilayer coupling K_1 and a strong reduction of $\tilde{K}_1$, respectively. These replacements have in common a change in the electron number provided by the transition metal atom, which changes the conduction band occupancy and the RKKY couplings. A double exchange coupling between the Gd magnetic moments through the 3d level of the transition metal naturally gives a change in the sign of the resulting coupling when the 3d level occupancy changes by one electron (see reference [37]), which may explain the observed behavior of the interbilayer couplings when the transition metal is replaced[6].

The compound GdTiGe is stable in both the CeFeSi-type (*P4/nmm*) and CeScSi-type (*I4/mmm*) structures, but its magnetic behavior depends strongly on the type of structure. GdTiGe (*P4/nmm*) is an A-type antiferromagnet while GdTiGe (*I4/mmm*) is a ferromagnet. Although the interbilayer couplings are expected to change because of the different topology, the intrabilayer couplings also change and are roughly twice as large in the CeScSi-type structure.

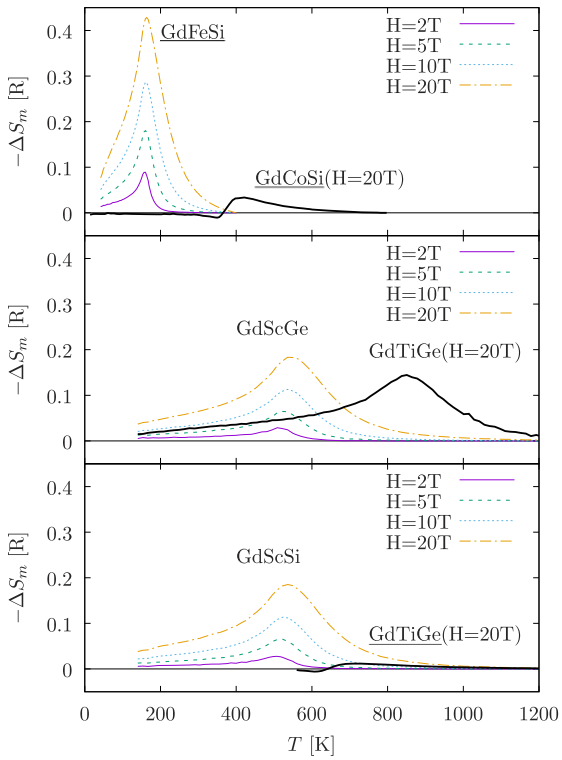

Figure 4. Magnetocaloric effect as a function of the temperature for different compounds and external magnetic fields. The underlined compound formulas correspond to the *P4/nmm* symmetry.

3. Magnetocaloric properties

We performed a mean-fied (MF) analysis and classical (CMC) and quantum Monte Carlo (QMC) calculations using the obtained magnetic couplings (see table 3) for each compound. We used the ALPS library (see references [38, 39]) for the numerical calculations with system sizes of up to $8 \times 8 \times 8$ magnetic moments. In figure 4 we present $-\Delta S_{\mathrm{m}} = S(0.1\,\mathrm{T}) - S(H)$ calculated numerically using quantum Monte Carlo, as a function of the temperature for four ferromagnetic and two antiferromagnetic compounds. The ferromagnetic compounds show a peak in $-\Delta S_{\mathrm{m}}$, for temperatures near the Curie temperature, whose height increases monotonically with increasing magnetic field. The maximum $-\Delta S_{\mathrm{m}}$ increases with decreasing T_{C} while the width of the peak follows an opposite trend. The antiferromagnetic compounds show a much lower overall intensity of the MCE and a change in the sign of $-\Delta S_{\mathrm{m}}$ near the Néel transition.

In the mean-field approximation the scaling $H \rightarrow g\mu_{\mathrm{B}}H/(k_{\mathrm{B}}T_{\mathrm{C}})$ (where $g = 2$ is the giromagnetic factor) and $T \rightarrow T/T_{\mathrm{C}}$ results in a universal curve for ΔS_{m} for the ferromagnetic compounds [40–43]. In the AFM compounds the maximum value of $-\Delta S_{\mathrm{m}}$ depends strongly on the value of the antiferromagnetic bilayer coupling (K_1 or $\tilde{K}_1$ depending on the crystal structure), since the Zeeman energy needs to be large enough to overcome it in order to be able to generate a sizable magnetization and the associated entropy change.

The scaling behavior is approximately followed in the CMC and the QMC calculations (see figure 5).

The maximum value of the entropy difference for a given external field is lower in CMC and QMC than in MF. This is due to the nature of the mean field solution in the paramagnetic state. At temperatures larger than the transition temperature T_{C} there are no correlations between spins in the MF approximation which leads to a maximal entropy and a lack of energy fluctuations. For $H \neq 0$ the energy fluctuations and the entropy are dominated by the level splitting induced by the external magnetic field which is accurately described in the MF approximation. For $T > T_{\mathrm{C}}$ and $H = 0$ the MF approximation overestimates the entropy but for $H \neq 0$ it results in a value similar to the one obtained using QMC. As a consequence, the MF approximation overestimates the entropy change when a magnetic field is applied.

The experimental entropy changes for GdFeSi, GdScGe and GdScSi are also shown in the insets of figure 5. At low (rescaled by $k_{\mathrm{B}}T_{\mathrm{C}}$) fields the experimental results (see reference [1] and references therein) are in very good agreement with the theory. The large field result, available for GdFeSi, is larger than what is expected from the theory, which could be due to additional magnetic degrees of freedom not

[6] We expect the magnetic couplings to be dominated by the hybridization of the Gd 5d orbitals with the conduction band rather than by the Gd 4f hybridization. A simple estimation using effective atomic orbitals indicates that the latter is at least two orders of magnitude smaller than the former.

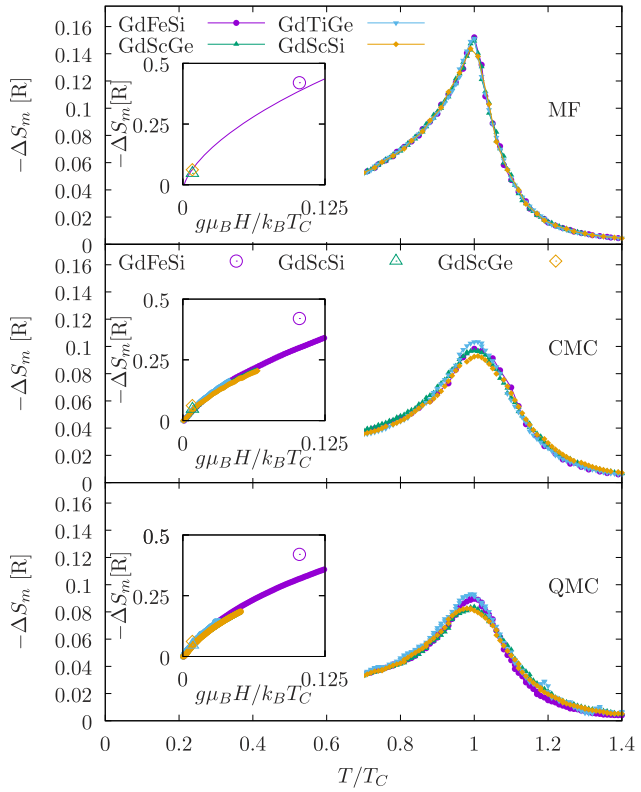

Figure 5. Magnetocaloric effect for different ferromagnetic compounds with both the temperature and the external magnetic field scaled by the corresponding T_C. The external magnetic field is $H = 2\,\mathrm{T}$ for GdFeSi and $H = 2\,\mathrm{T}(T_C/T_C^{\mathrm{GdFeSi}})$ for the other compounds. The insets show the entropy change as a function of the rescaled field at T_C. The open symbols correspond to experimental results with the magnetic field scaled by the experimental transition temperature (see reference [1] and references therein).

considered in our model (associated with the conduction band electrons).

4. Conclusions

We studied the magnetocaloric properties of Gd based RTX compounds having the CeScSi-type or CeFeSi-type crystal structures. Based on density functional theory calculations we obtained the ground state magnetic configuration and the exchange couplings of a simplified magnetic Hamiltonian. The lowest energy magnetic configurations obtained were in agreement with the available experimental data and the calculated transition temperatures consistent with the reported values. We found a weak dependence of the magnetic properties upon Si $\leftrightarrow$ Ge replacement but a strong dependence of the interbilayer exchange coupling with the replacements Fe $\rightarrow$ Co and Ti $\rightarrow$ Sc that can even lead to a change of its sign and of the magnetic ground state configuration. The replacement of Si by the isoelectronic Ge produces only small changes in the magnetic couplings.

A wide range of RTX compounds that share the CeFeSi-type crystal structure present the same qualitative change in the transition temperatures upon T replacement and X replacement (see table 4).

Table 4. Magnetic transition temperatures for compounds with the CeFeSi-type crystal structure. Shaded cells correspond to Curie temperatures.

	Ce	Nd	Sm	Gd	Tb	Dy	Ho	Er	Tm
RTiSi	—	—	—	400	286	170	95	50	20
RTiGe	—	150	260	412	270	170	115	41	15
RFeSi	—	25	40	118	125	110	29	22	—
RCoSi	8.8	7	15	175	140	—	—	—	—
RCoGe	5	8	—	—	—	—	—	—	—

We also studied the magnetocaloric properties of the R = Gd compounds and found a universal behavior of the magnetocaloric effect as a function of the temperature for the ferromagnetic compounds when the external magnetic field and the temperature are scaled by the transition temperature of each compound. This result, which is exact in the MF theory, and approximate in CMC and QMC sets a limit to the maximum MCE that can be expected in these compounds for a given T_C and external magnetic field.

Acknowledgments

We acknowledge financial support from PICT 2016-0204.

ORCID iDs

Daniel J García https://orcid.org/0000-0001-6777-9184
Verónica Vildosola https://orcid.org/0000-0002-7412-516X
Pablo S Cornaglia https://orcid.org/0000-0003-4991-6573

References

[1] Gupta S and Suresh K G 2015 Review on magnetic and related properties of RTX compounds *J. Alloys Compd.* **618** 562–606
[2] Cremades E, Gómez-Coca S, Aravena D, Alvarez S and Ruiz E 2012 Theoretical study of exchange coupling in 3D-Gd complexes: large magnetocaloric effect systems *J. Am. Chem. Soc.* **134** 10532–42
[3] Liu X B, Altounian Z, Han X, Poudyal N and Ping Liu J 2013 Magnetic state and exchange interaction in GdScGe: Ab initio study *J. Appl. Phys.* **113** 17E103
[4] Liu X B and Altounian Z 2010 First-principles calculation on the Curie temperature of GdFeSi *J. Appl. Phys.* **107** 09E103
[5] Talakesh S and Nourbakhsh Z 2017 The density functional study of structural, electronic, magnetic and thermodynamic properties of XFeSi (X=Gd, Tb, La) and GdRuSi compounds *J. Supercond. Novel Magn.* **30** 2143–58
[6] Gottschall T *et al* 2019 Magnetocaloric effect of gadolinium in high magnetic fields *Phys. Rev.* B **99** 134429
[7] Pecharsky A, Gschneidner K Jr and Pecharsky V 2003 The giant magnetocaloric effect of optimally prepared $Gd_5Si_2Ge_2$ *J. Appl. Phys.* **93** 4722–8
[8] Pecharsky V K and Gschneidner K A Jr 1999 Magnetocaloric effect and magnetic refrigeration *J. Magn. Magn Mater.* **200** 44–56

[9] Du J, Zheng Q, Li Y, Zhang Q, Li D and Zhang Z 2008 Large magnetocaloric effect and enhanced magnetic refrigeration in ternary Gd-based bulk metallic glasses *J. Appl. Phys.* **103** 023918

[10] Luo X-M, Hu Z-B, Lin Q-f, Cheng W, Cao J-P, Cui C-H, Mei H, Song Y and Xu Y 2018 Exploring the performance improvement of magnetocaloric effect based Gd-exclusive cluster Gd_{60} *J. Am. Chem. Soc.* **140** 11219–22

[11] Guillou F, Pathak A, Hackett T, Paudyal D, Mudryk Y and Pecharsky V K 2017 Crystal, magnetic, calorimetric and electronic structure investigation of $GdScGe_{1-x}Sb_x$ compounds *J. Phys.: Condens. Matter* **29** 485802

[12] Pecharsky V K and Gschneidner K A Jr 1997 Giant magnetocaloric effect in $Gd_5(Si_2Ge_2)$ *Phys. Rev. Lett.* **78** 4494

[13] Wlodarczyk P, Hawelek L, Zackiewicz P, Roy T R, Chrobak A, Kaminska M, Kolano-Burian A and Szade J 2015 Characterization of magnetocaloric effect, magnetic ordering and electronic structure in the GdFe1-xCoxSi intermetallic compounds *Mater. Chem. Phys.* **162** 273–8

[14] Skorek G, Deniszczyk J, Szade J and Tyszka B 2001 Electronic structure and magnetism of ferromagnetic GdTiSi and GdTiGe *J. Phys.: Condens. Matter* **13** 6397

[15] Couillaud S, Gaudin E, Franco V, Conde A, Pöttgen R, Heying B, Rodewald U C and Chevalier B 2011 The magnetocaloric properties of GdScSi and GdScGe *Intermetallics* **19** 1573–8

[16] Napoletano M, Canepa F, Manfrinetti P and Merlo F 2000 Magnetic properties and the magnetocaloric effect in the intermetallic compound GdFeSi *J. Mater. Chem.* **10** 1663–5

[17] Blaha P, Schwarz K, Madsen G K H, Kvasnicka D and Luitz J 2001 *WIEN2K, An Augmented Plane Wave + Local Orbitals Program for Calculating Crystal Properties* (Austria: Techn. Universität Wien)

[18] Perdew J P, Burke K and Ernzerhof M 1996 Generalized gradient approximation made simple *Phys. Rev. Lett.* **77** 3865

[19] Anisimov V I, Solovyev I V, Korotin M A, Czyżyk M T and Sawatzky G A 1993 Density-functional theory and NiO photoemission spectra *Phys. Rev.* B **48** 16929–34

[20] Yin Z and Pickett W 2006 Stability of the Gd magnetic moment to the 500GPa regime: an LDA+U correlated band method study *Phys. Rev.* B **74** 205106

[21] Petersen M, Hafner J and Marsman M 2006 Structural, electronic and magnetic properties of Gd investigated by DFT+ U methods: bulk, clean and H-covered (0001) surfaces *J. Phys.: Condens. Matter* **18** 7021

[22] Facio J I, Betancourth D, Pedrazzini P, Correa V F, Vildosola V, García D J and Cornaglia P S 2015 Why the Co-based 115 compounds are different: the case study of $GdMIn_5$ (M=Co, Rh, Ir) *Phys. Rev.* B **91** 014409

[23] Betancourth D, Facio J, Pedrazzini P, Jesus C, Pagliuso P, Vildosola V, Cornaglia P S, García D and Correa V 2015 Low-temperature magnetic properties of GdCoIn5 *J. Magn. Magn Mater.* **374** 744–7

[24] Betancourth D, Correa V, Facio J I, Fernández J, Vildosola V, Lora-Serrano R, Cadogan J, Aligia A, Cornaglia P S and García D 2019 Magnetostriction reveals orthorhombic distortion in tetragonal Gd compounds *Phys. Rev.* B **99** 134406

[25] Facio J I, Betancourth D, Bolecek N C, Jorge G A, Pedrazzini P, Correa V F, Cornaglia P S, Vildosola V and García D J 2016 Lattice specific heat for the RMIn5 (R=Gd, La, Y; M= Co, Rh) compounds: non-magnetic contribution subtraction *J. Magn. Magn Mater.* **407** 406–11

[26] Welter R 1994 Propriétés structurales et magnétiques de siliciures et germaniures ternaires RTX et RT2X2: R=Ca, Ba, Sc, Y, La et lanthanoïdes; T=Mn et métaux des groupes 8 à 10 *PhD Thesis* (Université Henri Poincaré-Nancy 1)

[27] Klosek V, Verniere A, Ouladdiaf B and Malaman B 2002 Magnetic properties of CeFeSi-type RTiSi compounds (R=Gd–Tm, Lu, Y) from magnetic measurements and neutron diffraction *J. Magn. Magn Mater.* **246** 233–42

[28] Welter R, Venturini G and Malaman B 1992 Magnetic properties of RFeSi (R=La-Sm, Gd-Dy) from susceptibility measurements and neutron diffraction studies *J. Alloys Compd.* **210** 49–58

[29] Welter R, Venturini G, Ressouche E and Malaman B 1994 Magnetic properties of RCoSi (R=La—Sm, Gd, Tb) compounds from susceptibility measurements and neutron diffraction studies *J. Alloys Compd.* **210** 279–86

[30] Nikitin S, Tskhadadze I, Telegina I, Morozkin A and Seropegin Y D 1998 Magnetic properties of rtige compounds *J. Magn. Magn Mater.* **182** 375–80

[31] Gaudin E, Matar S F, Pöttgen R, Eul M and Chevalier B 2011 Drastic change of the ferromagnetic properties of the ternary germanide GdTiGe through hydrogen insertion *Inorg. Chem.* **50** 11046–54

[32] Nikitin S, Ovtchenkova I, Skourski Y V and Morozkin A 2002 Magnetic properties of ternary scandium rare earth silicides and germanides *J. Alloys Compd.* **345** 50–3

[33] Yosida K 1957 Magnetic properties of Cu–Mn alloys *Phys. Rev.* **106** 893–8

[34] Kasuya T 1956 A theory of metallic ferro- and antiferromagnetism on Zener's model *Prog. Theor. Phys.* **16** 45–57

[35] Ruderman M A and Kittel C 1954 Indirect exchange coupling of nuclear magnetic moments by conduction electrons *Phys. Rev.* **96** 99–102

[36] Welter R, Vernière A, Venturini G and Malaman B 1999 High rare earth sublattice ordering temperatures in new CeFeSi-type RTiGe (R=La-Nd, Sm) compounds *J. Alloys Compd.* **283** 54–8

[37] Oropesa W G C, Encina S, Pedrazzini P, Correa V F, Sereni J G, Vildosola V, García D J and Cornaglia P S 2020 Minimal model for the magnetic phase diagram of CeTi1−xScxGe, GdFe1−xCoxSi, and related materials *J. Magn. Magn. Mater.* **503** 166614

[38] Albuquerque A *et al* 2007 The ALPS project release 1.3: Open-source software for strongly correlated systems *J. Magn. Magn Mater.* **310** 1187–93

[39] Bauer B 2011 The ALPS project release 2.0: open source software for strongly correlated systems *J. Stat. Mech.: Theory Exp.* **2011** P05001

[40] Bonilla C M, Herrero-Albillos J, Bartolomé F, García L M, Parra-Borderías M and Franco V 2010 Universal behavior for magnetic entropy change in magnetocaloric materials: an analysis on the nature of phase transitions *Phys. Rev.* B **81** 224424

[41] Franco V, Conde A, Romero-Enrique J and Blázquez J 2008 A universal curve for the magnetocaloric effect: an analysis based on scaling relations *J. Phys.: Condens. Matter* **20** 285207

[42] Smith A, Nielsen K K and Bahl C R 2014 Scaling and universality in magnetocaloric materials *Phys. Rev.* B **90** 104422

[43] Biswas A, Chandra S, Samanta T, Ghosh B, Datta S, Phan M, Raychaudhuri A, Das I and Srikanth H 2013 Universality in the entropy change for the inverse magnetocaloric effect *Phys. Rev.* B **87** 134420